0013-4651/2016/163(4)/H3145/7/$33.00

JES Focus Issue Honoring Allen J. Bard

Electrochemical Detection of Nanoparticle Collision by Reduction of Silver Chloride

Rui Hao, Yunshan Fan, and Bo Zhang[z]

Department of Chemistry, University of Washington, Seattle, Washington 98195, USA

We report a new detection scheme to detect and study discrete collisional events of single metal nanoparticles on a carbon ultramicroelectrode (UME). Detection of single nanoparticle collision is based on rapid electrocatalytic reduction of silver chloride (AgCl) on metal nanoparticle surfaces when they diffuse and make electrical contacts with a AgCl-modified carbon UME substrate. Single collisional events can be recorded as individual millisecond current pulses on a carbon UME by a simple square wave voltage waveform. Detections of both 80-nm silver and 4-nm gold nanoparticles are demonstrated in this work. This method is simple yet powerful and allows continuous recording of nanoparticle collision events for hours. Moreover, this method uses surface-supported solid AgCl and does not involve added redox species in the bulk solution. Therefore, nanoparticle stability can be less affected by the presence of other redox species, such as hydrazine.
 [DOI: 10.1149/2.0191604jes]

Manuscript submitted November 2, 2015; revised manuscript received December 22, 2015. Published January 6, 2016. *This paper is part of the JES Focus Issue Honoring Allen J. Bard.*

In this report, we demonstrate the use of electrocatalytic reduction of silver chloride (AgCl) as a unique approach for studying single-nanoparticle collision on an ultramicroelectrode (UME). The transformation between Ag metal and AgCl is a key reaction in electrochemistry and particularly in the popular Ag/AgCl reference electrodes.[1,2] Reduction of AgCl on the silver metal surface involves direct reduction of Ag^+ with a minimal overpotential.[2] Reduction of solid AgCl on other conductive substrates, such as carbon, however, can be sluggish and may require a significant overpotential to reach an appreciable rate. Under relatively low overpotentials, AgCl deposited on a carbon UME can be quickly reduced back to silver metal and Cl^- when a metal (e.g., Ag or Au) nanoparticle collides onto the UME giving rise to an easily detectable amperometric signal. A thin film of AgCl deposit can be obtained by oxidizing electroplated or thermally-evaporated silver on a carbon UME in a Cl^- containing solution and scattered AgCl patches can be formed by simply oxidizing surface-adsorbed silver nanoparticles in the presence of Cl^-. One can then use this approach to detect and study single nanoparticle collisions on a carbon UME. This method uses only a thin film deposit of AgCl to detect single nanoparticles and does not involve extra redox species, such as hydrazine, in the bulk solution. In addition, it enables continuous recording of single collision events for hours using a simple square wave voltage waveform.

Metal nanoparticles are useful materials in numerous scientific and technological areas due to their unique catalytic,[3–5] optical,[6] and biochemical properties.[7–9] Single-particle investigation allows complete removal of ensemble averaging and thus offers tremendous potential in understanding true structure-function relationship in these areas. Single-particle experiments have been reported in the literature[10–12] and representative methods include the use of fluorescence to study nanoparticle catalysis,[13,14] the use of surface plasmon spectroscopy to record single-particle electrochemistry,[12,15–20] coupled optical-electrochemical 3D microscopies,[21] single-particle voltammetry on a nanoelectrode,[22–26] nanoelectrolyte confinement method for detection of catalytic nanoparticles,[27] and single-particle collision on an UME.[28–40] Single-particle collision is a unique approach due to its simplicity and fast speed allowing hundreds of nanoparticle events recorded in minutes. Previous studies have involved two popular detection strategies: electrochemical amplification (EA),[29,32,33] and direct oxidation or reduction of nanoparticles.[28,30,41,42]

The EA scheme utilizes an enhanced electrochemical rate of a redox species on a metal nanoparticle compared to the surface of an UME and detects single particles when they collide on the electrode.[32] We have reported the use of fast scan cyclic voltammetry (FSCV) to detect and analyze single particles.[43] One challenge of the EA scheme is that the UME surface can be quickly occupied with thousands of particles losing its detection capacity. Stevenson and coworkers have used a mercury-modified UME which refreshes its surfaces by quickly deactivating metal nanoparticles.[34,35] Direct oxidation and reduction of nanoparticles, on the other hand, can provide useful information on particle size and composition. However, it may be challenging to detect very small metal nanoparticles and clusters due to a limited number of electrons involved in the faradaic reaction when very small particles are studied.

Our approach in this work is based on reduction of AgCl on a carbon UME and is schematically illustrated in Figure 1 (top panel). A constant voltage, e.g., −100 mV vs Ag/AgCl, is applied on the carbon UME at which the reduction of AgCl is kinetically limited. When single metal nanoparticles (e.g., Ag or Au) collides on the electrode surface, AgCl can be rapidly reduced back to silver and Cl^- ions on the particle surfaces resulting in millisecond amperometric signal, as shown in the bottom panel. The current amplitude and duration can be affected by several key factors such as the size of the AgCl deposit, the holding potential, and the nanoparticle size and surface property. We anticipate that this method can be useful to the study of electrochemical reduction of nanoscale AgCl on metals. Other insoluble species, such as many halide salts of Ag^+, Pb^{2+}, and $(Hg_2)^{2+}$, may also be used as indicator redox species for single particle collision.

Experimental

Chemicals and materials.—Methanol (Sigma Aldrich), potassium chloride (KCl, Fisher Scientific), ferrocene methanol (FcMeOH, Aldrich 97%), potassium ferricyanide ($K_3Fe(CN)_6$, Sigma-Aldrich 99%), potassium ferrocyanide ($K_4Fe(CN)_6$, Fluka 99.5%), hydrazine (anhydrous 98%, Sigma Aldrich), monobasic potassium phosphate (KH_2PO_4, J. T. Baker), dibasic potassium phosphate (K_2HPO_4, J. T. Baker), gold chloride trihydrate ($HAuCl_4 \cdot 3H_2O$, Sigma Aldrich), trisodium citrate (J. T. Baker), citric acid (Fisher Scientific), sodium borohydride (Sigma Aldrich), 2-allylphenol (Sigma Aldrich), ammonium hydroxide (Fisher Scientific), 80 nm silver nanoparticles (nanoComposix, Inc. San Diego, CA), were all used as received from the manufacturer. All aqueous solutions were made using deionized water (>18 MΩ · cm) obtained from a Barnstead Nanopure water purification systems.

Preparation of carbon UMEs.—The preparation of the carbon UMEs was based on a previously published procedure.[44] First, a piece of 7 μm carbon fiber was sealed in borosilicate tubings (O.D. 1.2 mm,

[z]E-mail: zhang@chem.washington.edu

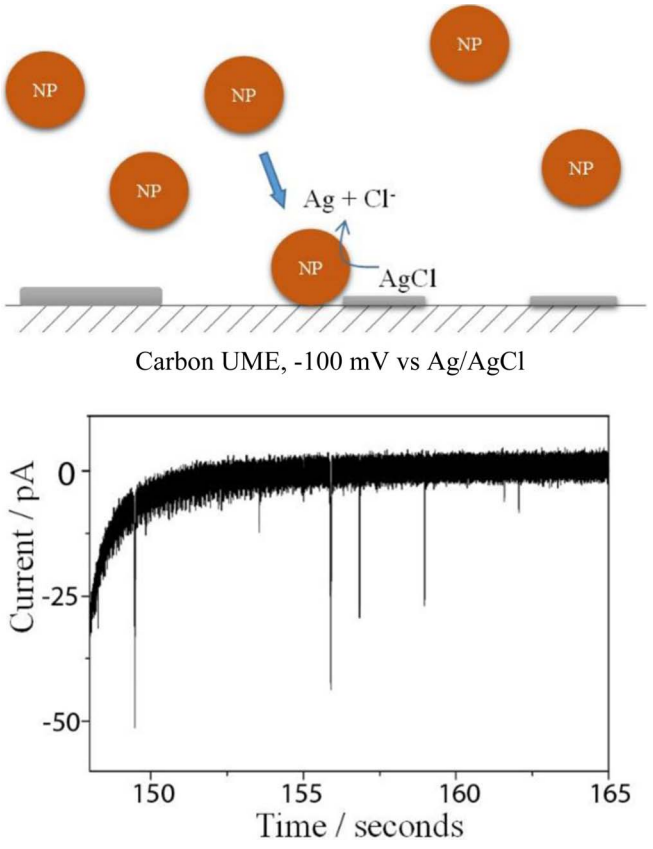

Figure 1. (Top panel) A cartoon showing detection of single-nanoparticle collision using AgCl reduction. (Bottom panel) A representative current-time trace showing detection of single metal nanoparticles on a carbon UME. The sharp current pulses are due to electrocatalytic reduction of AgCl on the surface of a metal nanoparticle after collision.

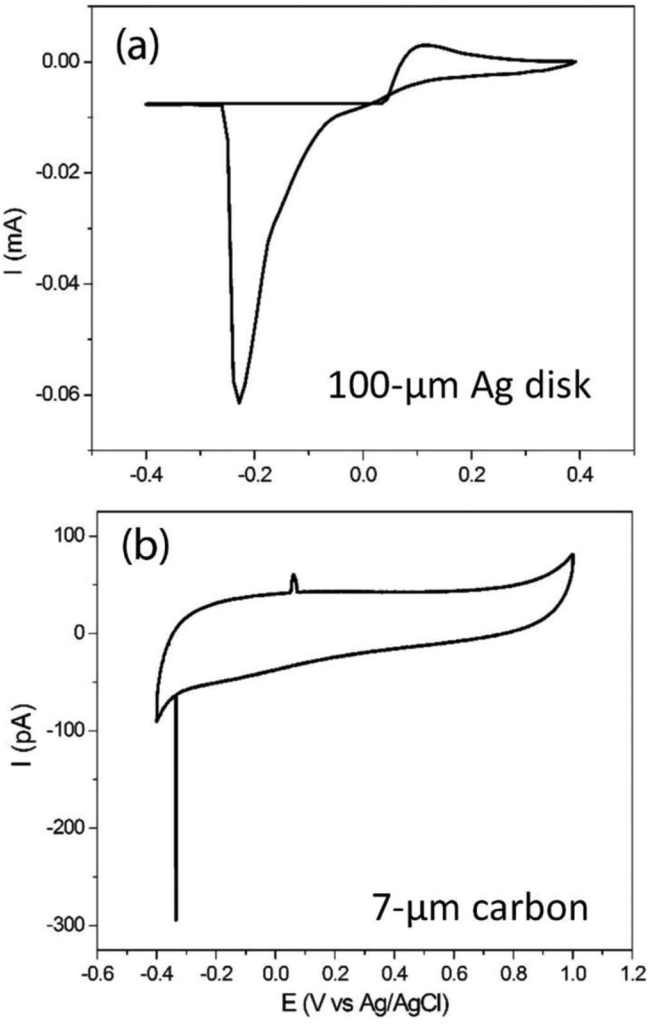

Figure 2. CV responses at 100 mV/s of a 100 µm silver disk electrode (a) and a 7 µm silver modified carbon UME (b) in 0.1 M KCl and 10 mM trisodium citrate. In (a), both the onset potentials for the oxidation of silver and the reduction of AgCl were close to 0 V vs Ag/AgCl indicating relatively small overpotentials. In (b), the reduction for AgCl on carbon did not start until the potential was scanned over −300 mV vs Ag/AgCl. This large overpotential is likely due to inactive electrocatalytic property of carbon.

I.D. 0.69 mm) by thermal pulling on a micropipette puller (Sutter instruments P-97). Then, a direct contact was made using silver paste (DuPont) and tungsten wire. A 5-mm portion of the carbon fiber should be left out of the capillary after the pulling. We then electrodeposited and cross-linked 2-allylphenol copolymer to insulate the carbon fiber. A H_2O/methanol (1:1) solution containing 0.90 mM 2-allylphenol was used for electrodeposition and the pH was adjusted to 9.0-9.2 by adding ammonium hydroxide. A +4 V potential (vs platinum wire counter electrode) was applied to the carbon fiber to deposit 2-allylphenol copolymer for 10 min. The polymer coating was then cured in an oven at 150 °C for 30 min. The electrodes would be cut to expose a fresh carbon surface by a stainless steel lancet or a glass knife before use.

Electrochemical measurements.—Steady-state CVs were recorded using a computer controlled Dagan Chem-Clamp voltammeter/amperometer and an in-house virtual instrumentation program written in LabView 8.5 (National instruments). A desktop Dell PC equipped with a PCI-6251(National Instruments) data acquisition card was used for date acquisition. Homemade and commercially available Ag/AgCl reference electrodes (Bioanalytical Sciences, Inc.) were used as reference electrode for all electrochemical data.

Synthesis of 4 nm gold nanoparticles.—Gold nanoparticles were synthesized by the reduction of $HAuCl_4$ by $NaBH_4$ in the presence of sodium citrate.[45] 200 ml of 2.5×10^{-4} M $HAuCl_4$ and sodium citrate aqueous solution was prepared in a flask. Then, 6 ml of 0.1 M $NaBH_4$ solution was rapidly injected into the flask while vigorous stirring and 4 nm Au nanoparticles formed instantly. The nanoparticles were collected by centrifuge and dispersed in a 2.5×10^{-4} M sodium citrate solution.

Electron microscopy.—TEM images were obtained on a FEI Tecnai G2 F20 microscope. SEM imaging was performed on a FEI XL830 Dual Beam system.

Results and Discussion

Reduction of AgCl on silver and carbon.—Figure 2a shows a cyclic voltammogram (CV) at 100 mV/s on a 100 µm diameter silver disk electrode in an aqueous solution containing 0.1 M KCl and 10 mM sodium citrate. The onset potential for silver oxidation is around +70 mV vs a homebuilt Ag/AgCl reference electrode while the onset potential for AgCl reduction is around -50 mV. There is a ~120 mV potential difference between oxidation and reduction peaks which may be partially due to a blocking effect of AgCl on the electrode.[46] This result confirms that reduction of AgCl on silver surface is fast and does not require significant overpotential.

In a second experiment, we first electrochemically deposited a small amount of silver on a 7 µm diameter disk-shape carbon UME

by applying a reduction potential of −600 mV vs Ag/AgCl for 100 s in a solution containing 10 μM $AgNO_3$. AgCl was then formed by electrochemically oxidizing the Ag in the presence of Cl^-. Figure 1b shows a CV recorded on the silver-modified carbon UME in 0.1 M KCl and 10 mM trisodium citrate. The oxidation of silver to AgCl had an onset potential of +80 mV vs Ag/AgCl, which is quite similar to that on the 100 μm diameter silver disk electrode. However, as shown in Figure 1b, the reduction of AgCl on the carbon UME did not start until the potential was scanned to around −330 mV and is now represented by a sharp current spike. In Figure 2b, the charges of the Ag oxidation spike and the AgCl reduction peak were both measured to be 0.21 pC, which correlated well. The large overpotential is likely due to an inefficient catalytic property of carbon for the reduction of AgCl and the sharp spike is likely caused by rapid reduction at this high overpotential after nucleation. Based on this significant potential difference, one can anticipate that the presence of metallic nanoparticle at or near to the AgCl deposit can act as an effective nucleation site for reduction of AgCl. Therefore, we propose to detect single-nanoparticle collision with a AgCl-modified carbon UME.

Detection of 80-nm silver nanoparticles.—Two methods were used to prepare a AgCl-modified carbon UME. The first method generates discrete patches of AgCl deposits by directly oxidizing 80 nm Ag nanoparticles on carbon at +400 mV vs Ag/AgCl in a nanoparticle solution containing 0.1 M KCl, and 10 mM trisodium citrate. This method is simple and allows nanoparticle detection in the same solution using a simple square pulse voltage program. AgCl can also be formed by first reducing $AgNO_3$ to form a thin silver film followed by oxidizing silver in a NaCl solution.

We first performed detection of single Ag nanoparticles on a 7 μm carbon UME in a solution containing 0.65 pM, 80 nm Ag nanoparticles, 0.1 M KCl, and 10 mM trisodium citrate using a square-wave voltage program: a constant voltage at +400 mV for 2 s, which oxidizes Ag particles to form individual AgCl patches on the carbon, followed by an 18 s reduction period at −100 mV vs AgCl to detect Ag nanoparticle collision. The TEM image in Figure S2 confirms the size and monodispersity of Ag particles. Figure 3a displays five 18 s detection traces for 80 nm citrate-capped Ag particles at an applied potential of −100 mV vs AgCl. Several individual sharp reduction spikes of ∼10 pA can be clearly observed on each trace. Figures 3b and 3c show current responses of single detection events as marked in traces 1 and 3, respectively. The duration of a particle collision event varies from 30 to 100 ms and the current spike is nearly symmetrical. The relatively longer event duration observed in this study is due to dissolution of AgCl, diffusion and subsequent reduction of Ag^+ ions on surface of silver nanoparticles. We analyzed the charge for the current spikes collected at −100 mV and the histogram is given in Figure 3d. The average charge in each current peak is about 69 ± 23.3 fC, which corresponds to a spherical Ag particle of ∼24 nm in diameter or the addition of a thin 0.7 nm layer of silver on the surface of an 80-nm diameter Ag particle. There are a few detection events with charge greater than 500 fC which may indicate the growth of larger nanostructures. The detection frequency is ∼6 particles/min which is nearly an order of magnitude lower than the frequency of 50 particles/min measured[47] from the silver nanoparticle stripping experiments (Figure S3). This low detection frequency supports our hypothesis that silver nanoparticles are detected only when they collide and stick to an electrode area where a AgCl patch is present. The number of discrete AgCl patches and their distribution on the UME are determined by the length of the oxidation half cycle.

Although AgCl is generally considered insoluble in water with a small solubility product constant, K_{sp}, of 1.8×10^{-10}, there is still a certain amount of free silver ions in the solution, which is calculated to be about 1.8 nM in 0.1 M KCl at equilibrium. According to the previous CV results, AgCl can hardly be reduced on carbon at a potential more positive than −300 mV vs Ag/AgCl. We believe the freely diffusing Ag nanoparticles can act as a nucleation site for AgCl reduction once they come in contact with carbon to an area close to a AgCl patch at −100 mV resulting in an accelerated dissolution and reduction of AgCl on Ag. Considering the diffusion coefficients of Ag^+ in water (1.485×10^{-5} cm^2/s)[48] and Ag^+ in solid AgCl (∼1×10^{-11} cm^2/s),[49] the electrochemical reduction of solid AgCl and thus detection of Ag nanoparticle collision should be strongly dependent on the supersaturated Ag^+ ions around AgCl nanosized patches. Direct conversion of the solid-state AgCl patch may still happen. However, it would not result in a sharp millisecond current response due to the very slow diffusion of Ag^+ in solid AgCl.

The detection of nanoparticle collision will be self-limiting after each 2-s anodic period at +400 mV as the AgCl would eventually be consumed by electrochemical reduction in the cathodic period or quickly dissolved due to fast radial-type diffusion and no more collisions would be detected at −100 mV. Hence, another 2 s oxidation at +400 mV was applied after the 18 s detection period in order to oxidize more Ag nanoparticles to regenerate more AgCl nanopatches. Continuous detection of single silver nanoparticles can thus be achieved by repeating this process. As a control experiment, we carried out the same detection scheme in a solution with no nanoparticles present. As shown in Figure S1, no detection spikes were observed.

Figure 4a shows detection traces for 80 nm Ag nanoparticles at different reduction potentials (−50, −100, −200, −300, and −600 mV vs Ag/AgCl) in each square wave program. The oxidation half-cycle was kept the same for each detection condition. The noise levels for detection traces at 0 mV, −50 mV, −100 mV, −200 mV, −300 mV were all around 3 pA. The significant higher noise level at −600 mV was due to the high baseline current at this high voltage. No detection events were observed at 0 mV (Figure S4) because the potential was insufficient to reduce AgCl even on silver metal surfaces. At −50 mV, nanoparticle detection spikes can be readily observed but the event frequency was relatively low. This low detection probability is likely due to insufficient driving force, and the result is consistent with the −50 mV onset potential for AgCl reduction on silver shown in Figure 1b. When the potential was further increased between −100 to −300 mV, single collision events with peak currents around 10 to 20 pA were clearly observed. Interestingly, no collision events were detected at −600 mV. We believe the absence of nanoparticle detection events is due to fast reduction of AgCl on carbon at this voltage which eliminates any possible AgCl patches previously present on carbon. Therefore, even though silver nanoparticles could still collide on carbon UME surfaces, no particles can be detected due to the absence of AgCl. Individual current spikes could again be observed when the electrode potential of the cathodic period of the squarewave was switched back to −300 mV. The absence of detection events at −600 mV further supports our hypothesis that nanoparticle detection is indeed due to the presence of AgCl (which should not exist at this very large overpotential). The result also confirms that the detection signals are not due to the direct reduction of AgCl or Ag_2O particles in solution because these particles should also be detected at this large potential.

To further verify the critical role of AgCl, we conducted electron microscopy experiments on a large 1 cm^2, 30 nm thick carbon film electrode supported on a glass coverslip. Figure 4b displays an SEM image of a carbon film electrode after applying a +400 mV potential for 2 s in 0.1 M KCl and 10 mM trisodium citrate solution containing 0.65 pM Ag nanoparticles. One can see sub-micrometer patches attached on the electrode surface which are likely nanoparticles of AgCl electrodeposited on carbon. Figure 4c shows the surface morphology of another carbon film electrode after applying 2 s oxidation potential at +400 mV vs Ag/AgCl in the same solution and then switching the potential to −100 mV for 20 s. Very bright Ag nanoparticles can be clearly distinguished from the surrounding gray particles that are similar to those observed in Figure 4b. These brighter silver nanoparticles are measured to be close to 80 nm. Therefore, we believe the gray particles in Figures 4b and 4c are AgCl and the brighter particles in Figure 3c are metallic Ag particles. The size of the nanoparticles in Figure 4c is consistent with the TEM results and our estimated minimum increase (e.g., 0.7 nm) in diameter based on the amperometry results.

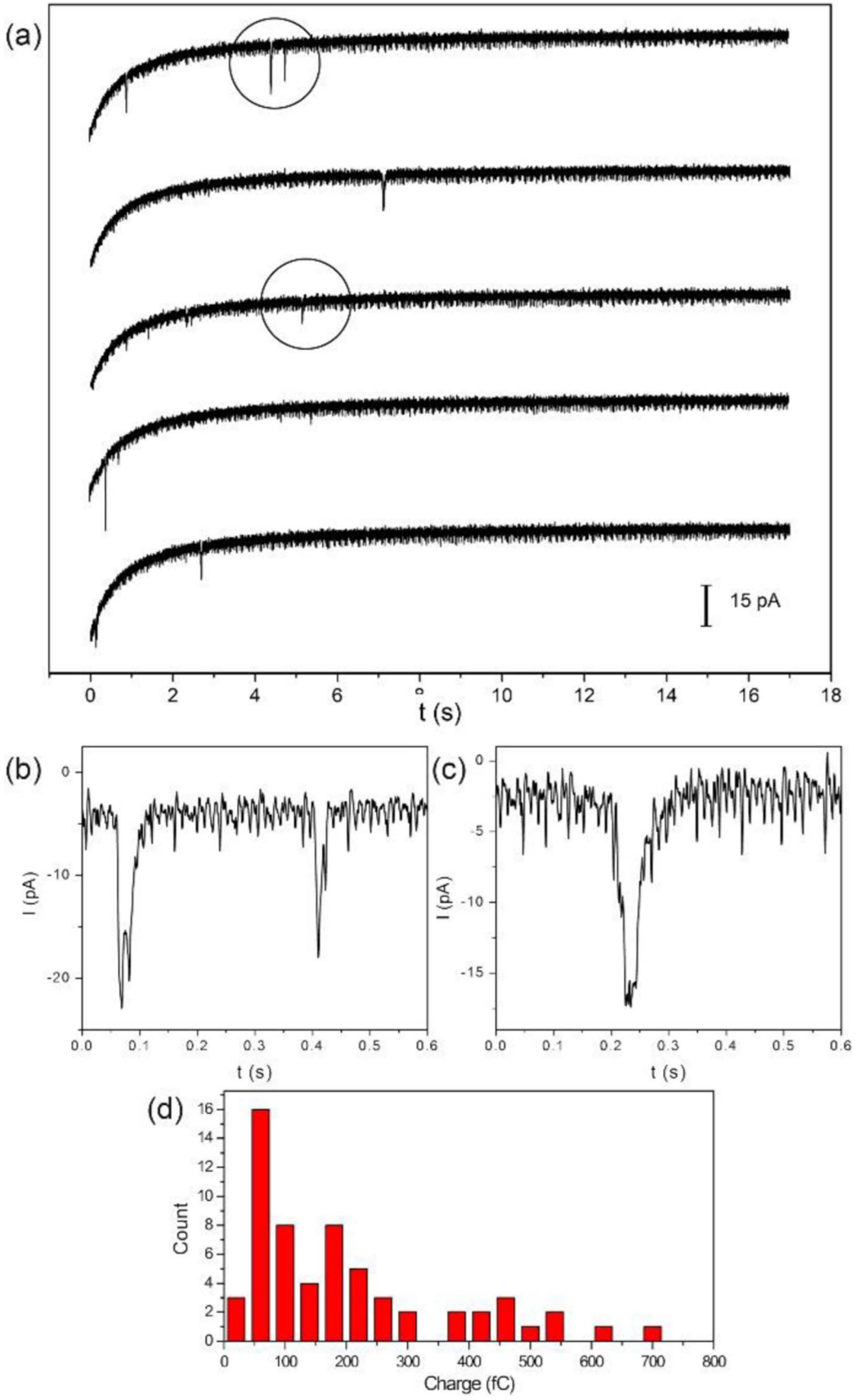

Figure 3. (a) Five *i-t* traces collected at −100 mV on a 7 μm AgCl modified carbon UME showing detection of single Ag nanoparticles in 0.1 M KCl and 10 mM trisodium citrate containing 0.65 pM 80 nm diameter Ag nanoparticles. Thin deposit of AgCl on carbon was obtained by in situ oxidation of Ag nanoparticles on carbon at +400 mV while the detection traces were collected at −100 mV. (b) and (c) are magnified views of the spikes indicated in (a). (d) A histogram showing the number of detected collisional events vs total charge integrated in each spike.

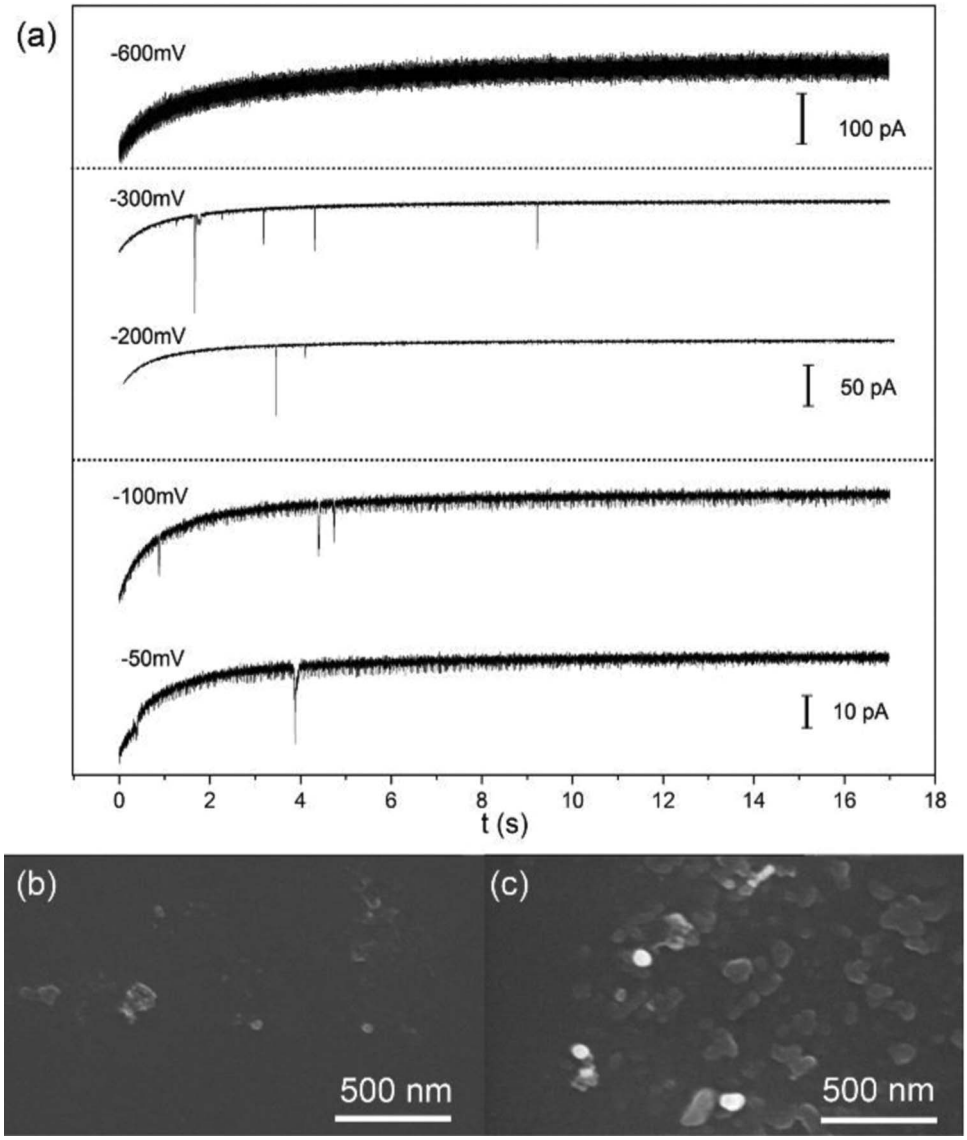

Figure 4. (a) Five amperometric traces collected on a 7 μm AgCl modified carbon UME showing detection of single collisional events of Ag nanoparticles in 0.1 M KCl and 10 mM trisodium citrate containing 0.65 pM 80 nm diameter Ag nanoparticles. The detection potential was varied at −50, −100, −200, −300 and −600 mV vs Ag/AgCl. (b) An SEM image of a AgCl modified carbon film electrode. AgCl modification was obtained by oxidizing Ag nanoparticles at +400 mV vs Ag/AgCl. (c) An SEM image of a AgCl modified carbon film electrode prepared as in (c) after detecting 80-nm Ag nanoparticles at −100 mV vs Ag/AgCl.

Detection of 4-nm gold nanoparticles.—AgCl-modified carbon UMEs can also be used to detect single collisional events of gold nanoparticles. A 7 μm carbon UME was modified with AgCl by first reducing $AgNO_3$ to form a thin silver film followed by oxidizing silver in a NaCl solution. The electrode was scanned in a 0.1 M KCl and 10 mM trisodium citrate solution until no oxidation/reduction spikes could be seen (Figure S8). The electrode was then placed in a new solution containing 0.1 M KCl and 10 mM trisodium citrate for detection of gold nanoparticles. Citric acid capped 4 nm gold nanoparticles were prepared according to the literature procedure.[43] Individual collision events were detected immediately after the addition of gold nanoparticles, as shown in Figure 5a. Apparently, the detection frequency is relatively low (3 particles /min) and the height of the current spikes, around 5 to 20 pA, is a bit smaller compared to previous detection events of 80 nm Ag nanoparticles possibly due to a smaller size of gold nanoparticles and different adhesion properties on carbon. Detailed plots of the current response are given in Figures 5b and 5c. Both of the current transients are around 10 ms wide and are significantly faster than that observed on Ag particles. Control experiments were also carried out by replacing the homemade Ag/AgCl electrode with a commercial Ag/AgCl. There is a small potential difference, <50 mV, for Ag^+ reduction on silver by using different Ag/AgCl reference electrodes according to the CV results. The detection potential was changed accordingly when a commercial reference electrode was used. To further confirm the detection mechanism, we also conducted experiments on bare carbon UME but no detection was found (Figure S9). The detection traces of gold nanoparticles with AgCl-modified carbon UME by using commercial Ag/AgCl reference electrode can be found in Figure S10, which shows no obvious differences compared to the results obtained using a homebuilt Ag/AgCl.

Conclusions

In summary, a new method has been demonstrated for electrochemical detection of single collision events of Ag and Au nanoparticles on a carbon ultramicroelectrode. This method is based on rapid reduction of AgCl on metal nanoparticle surfaces when a nanoparticle diffuse and collide on the carbon UME. This method eliminates the addition and presence of extra redox molecules, such as hydrazine, in the bulk

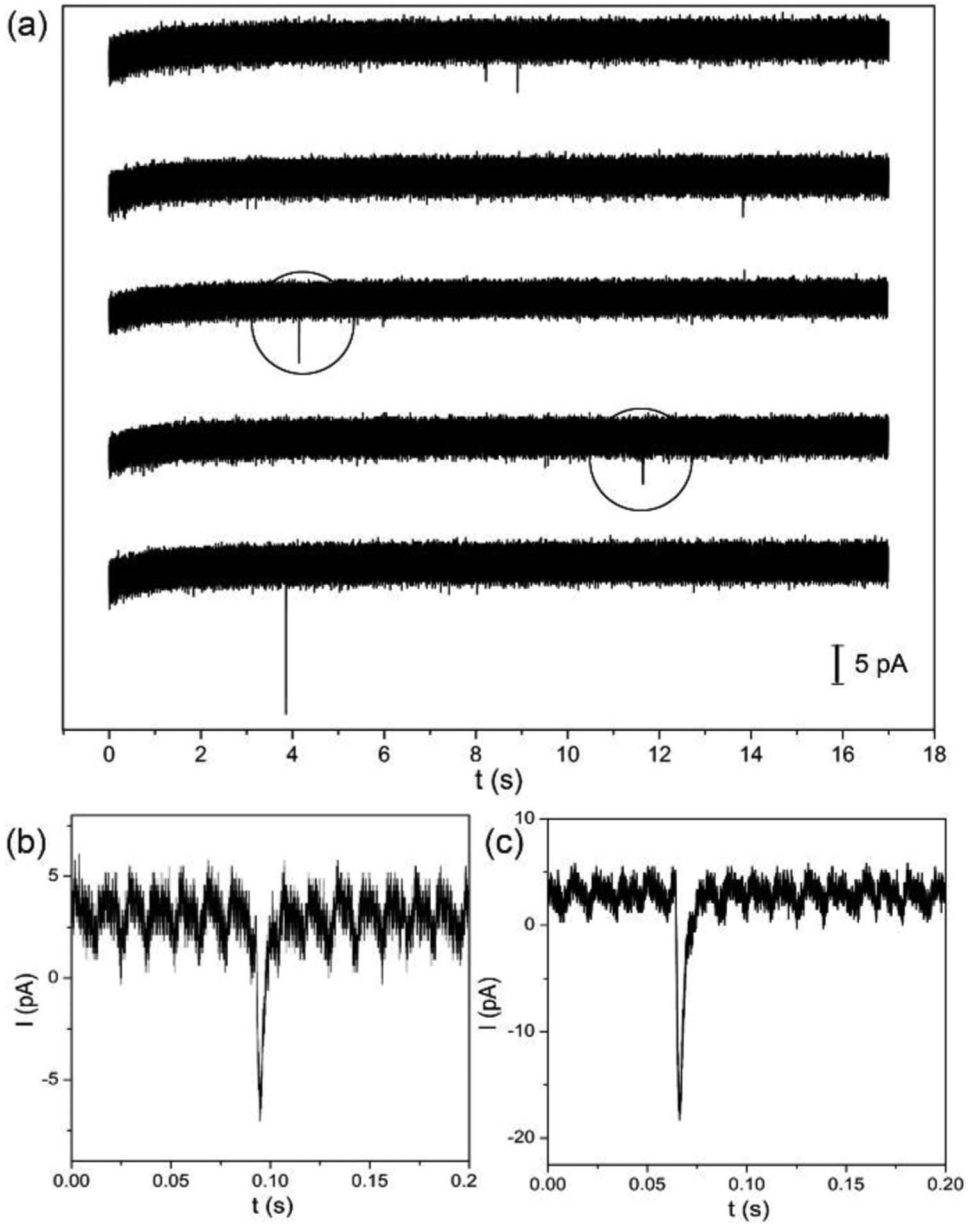

Figure 5. (a) Five amperometric traces collected at -100 mV on a 7 μm AgCl modified carbon UME showing detection of single collisional events of Au nanoparticles in 0.1 M KCl and 10 mM trisodium citrate containing 6 pM 4 nm diameter Au nanoparticles. A AgCl-modified carbon UME was prepared by electrochemically oxidizing silver metal at +400 mV in 0.1 M KCl. (b) and (c) are magnified views of the spikes indicated in (a).

solution. Therefore, the chemical stability of analyte nanoparticles can be enhanced due to less redox species presence. This method enables fast and continuous recording of single collision events of silver nanoparticles for extended time using a square wave potential program. Silver nanoparticles are first oxidized on carbon UME in the presence of Cl^- ions to form discrete patches of AgCl. Reduction of AgCl takes place in the subsequent cathodic half-cycle when a silver nanoparticle collides with the UME in the vicinity of the AgCl. Detection of both 80-nm silver and 4-nm gold nanoparticles has been demonstrated although this method can likely be extended to nanoparticles of other metals.

Acknowledgments

The authors gratefully acknowledge financial support from the Defense Threat Reduction Agency (DTRA) (HDTRA1-11-1-0005) and the AFOSR MURI (FA9550-14-1-0003). Part of this work was conducted at the University of Washington NanoTech User Facility, a member of the National Science Foundation, National Nanotechnology Infrastructure Network (NNIN).

References

1. G. A. Linhart, *J. Am. Chem. Soc.*, **41**, 1175 (1919).
2. H. M. Spencer, *J. Am. Chem. Soc.*, **54**, 3647 (1932).
3. S. Guo and E. Wang, *Nano Today*, **6**, 240 (2011).
4. C. Wang, H. Daimon, Y. Lee, J. Kim, and S. Sun, *J. Am. Chem. Soc.*, **129**, 6974 (2007).
5. Y. Liu, R. He, Q. Zhang, and S. Chen, *J. Phys. Chem. C*, **114**, 10812 (2010).
6. K. L. Kelly, E. Coronado, L. L. Zhao, and G. C. Schatz, *J. Phys. Chem. B*, **107**, 668 (2003).
7. M. Rai, A. Yadav, and A. Gade, *Biotechnol. Adv.*, **27**, 76 (2009).
8. R. Hao, R. Xing, Z. Xu, Y. Hou, S. Gao, and S. Sun, *Adv. Mater.*, **22**, 2729 (2010).
9. C. J. Murphy, A. M. Gole, J. W. Stone, P. N. Sisco, A. M. Alkilany, E. C. Goldsmith, and S. C. Baxter, *Accounts Chem. Res.*, **41**, 1721 (2008).
10. S. E. F. Kleijn, S. C. S. Lai, M. T. M. Koper, and P. R. Unwin, *Angew. Chemie-International Ed.*, **53**, 3558 (2014).

11. W. Wang and N. Tao, *J. Anal. Chem.*, **86**, 2 (2014).
12. J. B. Sambur and P. Chen, *Annu. Rev. Phys. Chem.*, **65**, 395 (2014).
13. X. Zhou, N. M. Andoy, G. Liu, E. Choudhary, K.-S. Han, H. Shen, and P. Chen, *Nat. Nanotechnol.*, **7**, 237 (2012).
14. N. M. Andoy, X. Zhou, E. Choudhary, H. Shen, G. Liu, and P. Chen, *J. Am. Chem. Soc.*, **135**, 1845 (2013).
15. C. P. Byers, B. S. Hoener, W.-S. Chang, M. Yorulmaz, S. Link, and C. F. Landes, *J. Phys. Chem. B*, **118**, 14047 (2014).
16. C. M. Hill, D. A. Clayton, and S. Pan, *Phys. Chem. Chem. Phys.*, **15**, 20797 (2013).
17. S. K. Dondapati, M. Ludemann, R. Mueller, S. Schwieger, A. Schwemer, B. Haendel, D. Kwiatkowski, M. Djiango, E. Runge, and T. A. Klar, *Nano Lett.*, **12**, 1247 (2012).
18. C. Jing, F. J. Rawson, H. Zhou, X. Shi, W.-H. Li, D.-W. Li, and Y.-T Long, *Anal. Chem.*, **86**, 5513 (2014).
19. X. Shan, I. Díez-Pérez, L. Wang, P. Wiktor, Y. Gu, L. Zhang, W. Wang, J. Lu, S. Wang, Q. Gong, J. Li, and N. Tao, *Nat. Nanotechnol.*, **7**, 668 (2012).
20. Y. Fang, W. Wang, X. Wo, Y. Luo, S. Yin, Y. Wang, X. Shan, and N. Tao, *J. Am. Chem. Soc.*, **136**, 12584 (2014).
21. A. N. Patel, A. Martinez-Marrades, V. Brasiliense, D. Koshelev, M. Besbes, R. Kuszelewicz, C. Combellas, G. Tessier, and F. Kanoufi, *Nano Lett.* (2015).
22. Y. Li, J. T. Cox, and B. Zhang, *J. Am. Chem. Soc.*, **132**, 3047 (2010).
23. Y. Yu, Y. Gao, K. K. Hu, P. Y. Blanchard, J. M. Noel, T. Nareshkumar, K. L. Phani, G. Friedman, Y. Gogotsi, and M. V. Mirkin, *Chemelectrochem*, **2**, 58 (2015).
24. J. Kim, B.-K. Kim, S. K. Cho, and A. J. Bard, *J. Am. Chem. Soc.*, **136**, 8173 (2014).
25. S. L. Chen and A. Kucernak, *J. Phys. Chem. B*, **108**, 3262 (2004).
26. P. Sun, F. Li, C. Yang, T. Sun, I. Kady, B. Hunt, and J. Zhuang, *J. Phys. Chem. C*, **117**, 6120 (2013).
27. M. Kang, D. Perry, Y.-R. Kim, A. W. Colburn, R. A. Lazenby, and P. R. Unwin, *J. Am. Chem. Soc.*, **137**, 10902 (2015).
28. W. Cheng and R. G. Compton, *Trac-Trends Anal. Chem.*, **58**, 79 (2014).
29. S. E. F. Kleijn, S. C. S. Lai, T. S. Miller, A. I. Yanson, M. T. M. Koper, and P. R. Unwin, *J. Am. Chem. Soc.*, **134**, 18558 (2012).
30. Y.-G. Zhou, N. V. Rees, and R. G. Compton, *Angew. Chemie-International Ed.*, **50**, 4219 (2011).
31. S. J. Kwon, F.-R. F. Fan, and A. J. Bard, *J. Am. Chem. Soc.*, **132**, 13165 (2010).
32. X. Xiao and A. J. Bard, *J. Am. Chem. Soc.*, **129**, 9610 (2007).
33. X. Xiao, F.-R. F. Fan, J. Zhou, and A. J. Bard, *J. Am. Chem. Soc.*, **130**, 16669 (2008).
34. R. Dasari, K. Tai, D. A. Robinson, and K. J. Stevenson, *ACS Nano*, **8**, 4539 (2014).
35. R. Dasari, D. A. Robinson, and K. J. Stevenson, *J. Am. Chem. Soc.*, **135**, 570 (2013).
36. S. E. Fosdick, M. J. Anderson, E. G. Nettleton, and R. M. Crooks, *J. Am. Chem. Soc.*, **135**, 5994 (2013).
37. A. D. Castañeda; T. M. Alligrant, J. A. Loussaert, and R. M. Crooks, *Langmuir*, **31**, 876 (2015).
38. B. M. Quinn, P. G. van 't Ho, and S. G. Lemay, *J. Am. Chem. Soc.*, **126**, 8360 (2004).
39. N. Perera, N. Karunathilake, P. Chhetri, and M. A. Alpuche-Aviles, *Anal. Chem.*, **87**, 777 (2015).
40. J. E. Dick, C. Renault, and A. J. Bard, *J. Am. Chem. Soc.* (2015).
41. E. J. E. Stuart, K. Tschulik, C. Batchelor-McAuley, and R. G. Compton, *ACS Nano*, **8**, 7648 (2014).
42. A. Yakushenko, D. Mayer, J. Buitenhuis, A. Offenhaeusser, and B. Wolfrum, *Lab Chip*, **14**, 602 (2014).
43. Z. Guo, S. J. Percival, and B. Zhang, *J. Am. Chem. Soc.*, **136**, 8879 (2014).
44. T. G. Strein and A. G. Ewing, *Anal. Chem.*, **64**, 1368 (1992).
45. N. R. Jana, L. Gearheart, and C. J. Murphy, *Langmuir*, **17**, 6782 (2001).
46. X. B. Jin, J. T. Lu, P. F. Liu, and H. Tong, *J. Electroanal. Chem.*, **542**, 85 (2003).
47. E. J. E. Stuart, Y.-G. Zhou, N. V. Rees, and R. G. Compton, *RSC Adv.*, **2**, 6879 (2012).
48. M. B. Kraichman and E. A. Hogge, *J. Phys. Chem.*, **59**, 986 (1955).
49. R. F. Reade and D. S. Martin, *J. Appl. Phys.*, **31**, 1965 (1960).